

Fragmentation cross sections of 2.1-GeV/nucleon ^{12}C and ^{16}O ions*

D. L. Cheshire, R. W. Huggett, D. P. Johnson,† W. V. Jones, S. P. Rountree,‡ and S. D. Verma
Department of Physics and Astronomy, Louisiana State University, Baton Rouge, Louisiana 70803

W. K. H. Schmidt

Max Planck Institut für Extraterrestrische Physik, 8046 Garching bei München, West Germany

R. J. Kurz

TRW Systems, Redondo Beach, California 90278

T. Bowen and E. P. Krider§

Department of Physics, University of Arizona, Tucson, Arizona 85721

(Received 11 February 1974)

A tungsten-scintillator ionization spectrometer (1000 g/cm² total depth) has been exposed to 2.1-GeV/nucleon ^{12}C and ^{16}O ions at the Bevatron. Fragmentations of the incident ions could be observed in a five-layer CsI target (each layer 9 g/cm² thick) and in five tungsten-scintillator layers (each 13 g/cm² thick). The number of fragmentations in each of these layers has been used to determine the total fragmentation cross sections. The Bradt-Peters overlap parameters are consistent with zero when calculated using these cross sections and a value of $r_0 = 1.25 \times 10^{-13}$ cm.

I. INTRODUCTION

A tungsten-scintillator ionization spectrometer (calorimeter) with a CsI target has been exposed to 2.1-GeV/nucleon ^{12}C and ^{16}O ions at the Bevatron. The exposure was made as part of a study of the cascade process initiated by heavy ions incident on heavy absorbers. We report here results of measurements of the total fragmentation cross sections of the beam particles in CsI and in tungsten. In this paper a fragmentation is considered to be any interaction which results in a change $\Delta Z \geq 1$ in the charge Ze of the incident ion.

Knowledge of the cross sections for the fragmentations of heavy nuclei is important for many cosmic-ray investigations currently underway. In measurements of the flux and charge composition of cosmic rays, it is often necessary to make corrections for interactions occurring in or above the detector. Information about the interactions of heavy nuclei with interstellar matter is necessary in order to obtain quantitative astrophysical information from cosmic-ray composition measurements made at or near the earth.¹⁻⁷ Also, information on the fragmentation of heavy nuclei is useful in developing theories of nucleosynthesis.⁸

The charge resolution of our apparatus was not sufficient to allow identification of individual fragments produced in interactions of the beam parti-

cles. Therefore, it was not possible to determine partial fragmentation cross sections. However, an interaction could be detected provided it involved a change in the charge of the primary particle. Consequently, we have measured the total cross section for interactions involving any process which results in a change $\Delta Z \geq 1$ in the charge Ze of the incident ion.

II. EXPERIMENTAL METHOD

The apparatus used in the experiment is shown, to scale, in Fig. 1. An event trigger was defined by scintillation counters TOF1, TOF2, and B1. The CsI section consisted of five CsI(Tl) crystal counters (CsI₁-CsI₅) viewed by separate photomultipliers. Each crystal was 2.0 cm (9 g/cm²) thick and was enclosed in a Plexiglas casing with walls 1 mm thick.

The tungsten-scintillator ionization spectrometer was divided into two parts. The first part had five "high resolution" modules (T_1 - T_5), each consisting of a thin tungsten layer and a sheet of plastic scintillator as shown in Fig. 2. The tungsten layers were 13 g/cm² or 1.85 radiation lengths (rl) in thickness. The thickness of each of the scintillators was 0.65 cm. Each module was viewed by a single photomultiplier. The second

part of the spectrometer consisted of eleven "thick" tungsten modules (T_6-T_{16}). These modules, shown in Fig. 2, consisted of 79 g/cm^2 (11.1 rl) of tungsten and three sheets of 0.65 cm thick plastic scintillator, arranged in alternating layers with 26.3 g/cm^2 (3.7 rl) of tungsten between each pair of scintillators. A photomultiplier on each of two opposite sides of the module viewed all three scintillators. The signals from the two photomultipliers were added electronically, and the resulting signal was used to determine the response of the module. Thus, although the ionization was sampled every 3.7 rl, the signal from a module was a measure of the average ionization over the entire module (11.1 rl). The thick tungsten modules (T_6-T_{16}) were used for a study, to

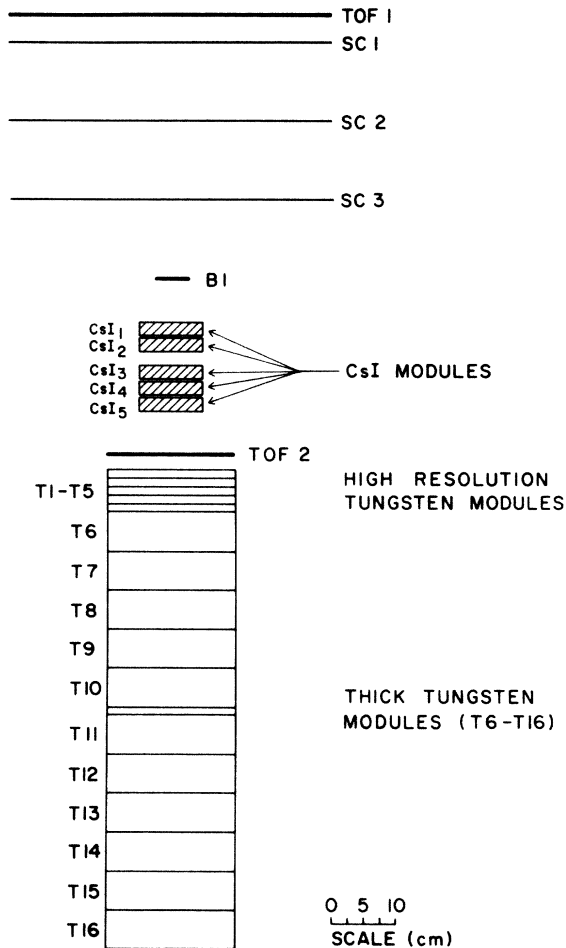


FIG. 1. Scale drawing of apparatus. SC1, SC2, and SC3 are wire spark chambers which were used in preliminary beam studies. TOF1, B1, and TOF2 are plastic scintillators which defined an event trigger.

be discussed in a subsequent paper, of the development of cascades initiated by heavy ions. Pulse heights from the scintillation counters, the CsI modules, and the tungsten modules were recorded on magnetic tape for each event.

III. DATA ANALYSIS

Our procedure was to look for the first interaction of an incident beam particle in either the CsI modules or in the high-resolution tungsten modules (T_1-T_5). The energy loss corresponding to the pulse height of the signal from each of these modules was converted into an equivalent particle number, i.e., the energy loss was expressed in units of the energy which would have been lost by some "standard particle." The standard particle was defined for the carbon run to be a particle which would lose $\frac{1}{36}$ as much energy as a relativistic ^{12}C ion. Correspondingly, for the ^{16}O run, the standard particle was defined as one which would lose $\frac{1}{64}$ as much energy as a relativistic ^{16}O ion.

An incident ion was considered to have interacted in the first module in which the energy loss was outside a selected "window" centered at 36 equivalent particles for the ^{12}C run and at 64 equivalent particles for the ^{16}O run. In order to eliminate events which had interacted in the material upstream of the CsI section, only those events with energy losses inside the window for the CsI₁ module were analyzed.

The number of interactions assigned to any module will clearly be influenced by the choice of window for that module. If the chosen window is too wide, then the energy loss for a true interaction may not fall outside the window, and the interaction will not be recognized. On the other

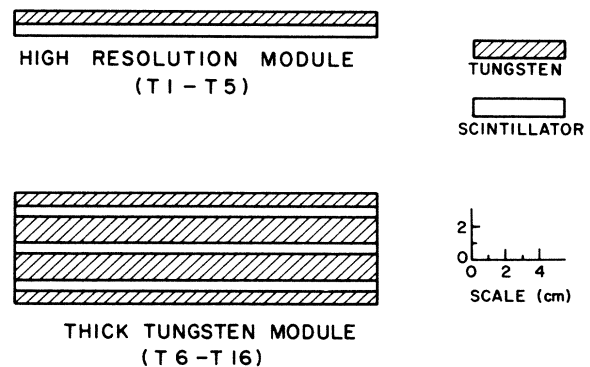


FIG. 2. Scale drawing of tungsten modules.

hand, if the window is too narrow, normal fluctuations in the energy loss of the incident ions will simulate interactions.

A typical energy-loss distribution for noninteracting particles in the first tungsten module (T_1) is shown in Fig. 3. The distribution, which we call a "noninteracting particle distribution," was obtained by requiring that the energy loss in each module other than T_1 be within the appropriate window. Hence, only events were selected in which an incident particle passed through all modules CsI_1-T_5 without interacting, according to the selection criterion applied to all the modules except T_1 . Two arbitrary windows, AA' and BB' , are indicated in Fig. 3. Of all noninteracting particles incident on T_1 , 2.4% have energy losses outside the window AA' , while only 0.9% have energy losses outside the wider window BB' . Therefore, use of window AA' , rather than the wider window BB' , will result in more interactions being assigned to the module. However, since the probability of an energy loss outside a window can be determined from the noninteracting particle distribution, empirical corrections can be made for simulated interactions. The results should then be independent of the choice of windows.

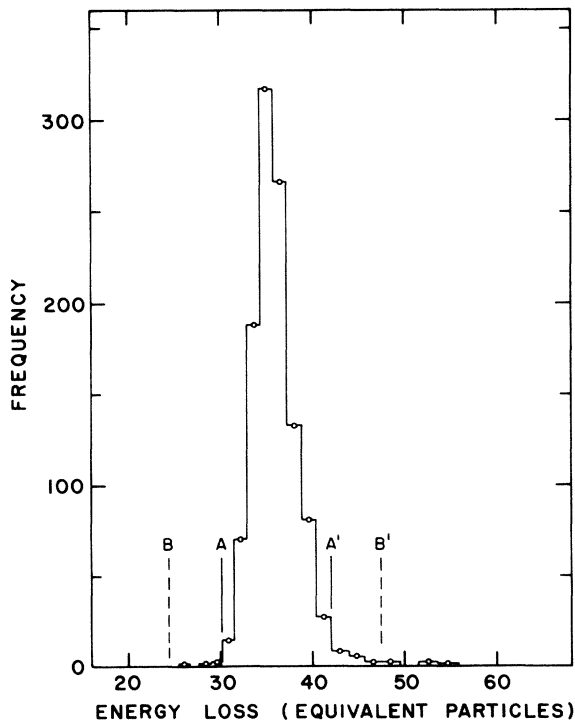


FIG. 3. Distribution of noninteracting ^{12}C ions (2.1-GeV/nucleon) in module T_1 . The solid lines AA' and the dashed lines BB' illustrate two arbitrary choices of windows for selecting noninteracting particles.

These corrections are sensitive to any contamination of the noninteracting particle distributions by interacting particles. Such contamination would occur for any interactions in which, because of fluctuations, the energy loss in each and every module downstream of the module being considered was within the selected window for a noninteracting particle. Clearly, this situation is more likely for the modules farther downstream, because they are followed by fewer modules. Such contamination appeared negligible for the CsI modules. However, the distributions for the last few tungsten modules were appreciably contaminated. Therefore, in making the corrections for simulated interactions, we have assumed the same noninteracting particle distributions for modules T_2-T_5 as for module T_1 . This assumption should be valid, since the responses (calibration constants, resolution, etc.) of all the tungsten modules were quite similar.

Our analysis is based on a determination of the module in which the first interaction of each incident ion occurred. The mean free path λ expressed in units of g/cm^2 was determined from the expression

$$N(i) = N_0(1 - e^{-t/\lambda}), \quad (1)$$

where $N(i)$ is the number of ions which have survived (not interacted) beyond the i th module, N_0 is the number of ions incident on the stack of modules, and t is the thickness of a module. The value of λ was determined from the slope of a straight-line fit to a semilogarithmic plot of $N(i)$ vs i . A least-squares technique was employed using $N(i)$ values as weighting factors. A maximum-likelihood calculation was also performed. The value

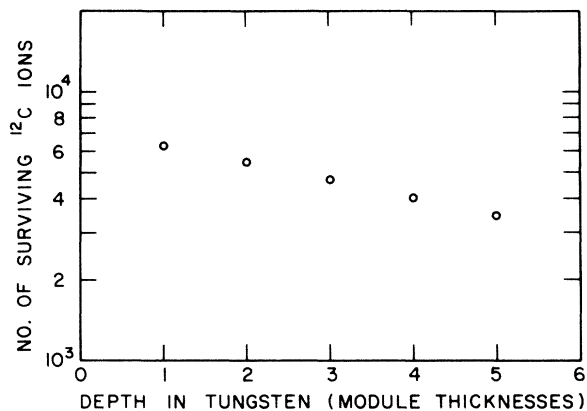


FIG. 4. Semilogarithmic plot of the number of surviving (noninteracting) ^{12}C ions as a function of depth in the tungsten modules T_1-T_5 . The slope of the line represents the reciprocal of the mean free path λ in units of the module thickness.

obtained for each λ differed by a negligible amount from that obtained by the least-squares technique. The error associated with each value of λ was taken to be the error obtained in the maximum-likelihood calculation. This error varied from $\pm 4\%$ to $\pm 9\%$ for various combinations of projectile, target, and window width.

The CsI and tungsten sections of the spectrometer were considered separately. A typical plot is illustrated in Fig. 4, which shows the number of surviving ^{12}C ions as a function of depth in the tungsten modules. The first and second CsI modules were not used in the determination of λ , in order to minimize boundary effects.^{9, 10} The first module was used to identify the incident particle. Interactions in the second module were identified, but the first point used in determining λ was the number of particles surviving CsI₂, i.e., incident on CsI₃. Similarly, interactions in the first tungsten module were identified, but the first data point used was the number of particles surviving T_1 , or incident on T_2 .

It was necessary to apply corrections to λ in order to account for interactions occurring in the Plexiglas casings of the CsI modules and in the scintillators of the tungsten modules. This was

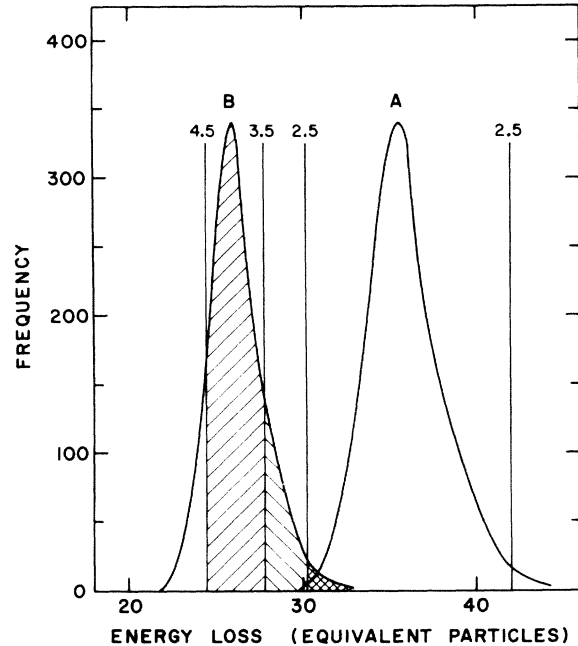


FIG. 5. Distribution of energy losses in the first tungsten module (T_1) for (A) noninteracting ^{12}C ions, (B) fragments produced in a $\Delta Z = 1$ interaction. Distribution (B) is normalized to the same height as distribution (A). The vertical lines indicate windows of varying widths about the noninteracting peak, and illustrate to what extent $\Delta Z = 1$ interactions will be missed if that window is used.

done, for example, for the ^{12}C beam in the tungsten modules by correcting the measured mean free path λ according to the relationship

$$\frac{t}{\lambda} = \frac{t_{\text{scin}}}{\lambda_{\text{scin}}} + \frac{t_{\text{W}}}{\lambda_{\text{W}}}, \quad (2)$$

where t is the thickness of a module, t_{scin} and t_{W} are, respectively, the thicknesses of scintillator and tungsten in a module, and λ_{scin} and λ_{W} are the corresponding mean free paths of the ^{12}C beam particles in scintillator and in tungsten. The value of λ_{scin} was calculated from the expression

$$\frac{1}{\lambda_{\text{scin}}} = \frac{P_{\text{C}}}{\lambda_{\text{C}}} + \frac{P_{\text{H}}}{\lambda_{\text{H}}}, \quad (3)$$

where P_{C} and P_{H} are, respectively, the partial weights ($P_{\text{C}} + P_{\text{H}} = 1$) of carbon and hydrogen in scintillator, while λ_{C} and λ_{H} are the corresponding mean free paths of ^{12}C beam particles in carbon and hydrogen. The values of λ_{C} and λ_{H} are based on measurements by Lindstrom *et al.*¹¹ for 2.1-GeV/nucleon beams of ^{12}C and ^{16}O . Corrections for the Plexiglas casings of the CsI modules were made in a similar manner. The error, which was due to uncertainties in the measured cross sections used in the calculations, was in all cases less than $\pm 1\%$.

The relationship of the interaction cross section σ to the mean free path λ is given by the expression

$$\sigma = \frac{A}{N_0 \lambda}, \quad (4)$$

where A is the atomic mass number of the absorber (184 for W, and 130 for CsI), and N_0 is Avogadro's number.

Window widths of 2.5, 3.5, and 4.5 times the full width at half-maximum (FWHM) of the noninteracting particle distribution for each module were used in the data analysis. For these window widths corrections had to be made for undetected $\Delta Z = 1$ interactions in the tungsten modules. The energy-loss distribution for noninteracting ^{12}C ions in T_1 shown in Fig. 3 has been represented by a smooth curve in Fig. 5. Also shown, normalized to the same height, is the energy-loss dis-

TABLE I. Cross sections σ and interaction mean free paths λ for 2.1-GeV/nucleon ^{12}C and ^{16}O nuclei in CsI and W targets.

Projectile	Target	σ (b)	λ (g/cm ²)
^{12}C	CsI	2.6 ± 0.1	83 ± 4
^{12}C	W	3.0 ± 0.1	101 ± 4
^{16}O	CsI	3.0 ± 0.2	71 ± 5
^{16}O	W	3.5 ± 0.3	87 ± 7

TABLE II. Cross sections σ obtained using three different window widths. The values in parentheses are obtained if corrections are not made for interactions simulated by energy loss fluctuations in the individual modules.

Projectile	Target	σ (b)		
		Window width (FWHM)		
		4.5	3.5	2.5
^{12}C	CsI	2.5(2.5)	2.6(2.7)	2.8(3.2)
^{12}C	W	3.0(3.2)	3.0(3.3)	3.0(3.7)
^{16}O	CsI	2.9(2.9)	3.0(3.1)	3.2(3.3)
^{16}O	W	3.5(3.9)	3.6(4.2)	3.4(4.5)

tribution expected for interactions in which $\Delta Z = 1$. The latter distribution was calculated assuming the same shape and fractional width as possessed by the noninteracting particle distribution. As illustrated in the figure, 88% of the $\Delta Z = 1$ interactions have an associated energy loss within the 4.5-FWHM window about the noninteracting particle peak and consequently will not be identified as interactions. Only 17% or 2%, respectively, of the $\Delta Z = 1$ interactions will not be detected if the 3.5- or 2.5-FWHM window is used.

The ratio of the cross section for $\Delta Z = 1$ interactions to the total cross section, for ^{12}C and ^{16}O heavy ion beams in CsI and W, was assumed to be the mean value measured by Lindstrom *et al.*,¹¹ for each of these heavy ions, in Cu and Pb targets. The fraction of all events in which a $\Delta Z = 1$ interaction occurred but was undetected in our analysis is given by the product of the percentage of undetected $\Delta Z = 1$ interactions times the ratio of the $\Delta Z = 1$ cross section to the total cross section. Corrections to our data for these undetected interactions were negligible for both heavy ion beams in the CsI target, but were as high as 10% for the tungsten target. This difference was due to the better energy resolution of the CsI modules, e.g., in a plot similar to Fig. 5 even the 4.5-FWHM window does not significantly overlap the $\Delta Z = 1$ energy-loss distribution. The error in these cor-

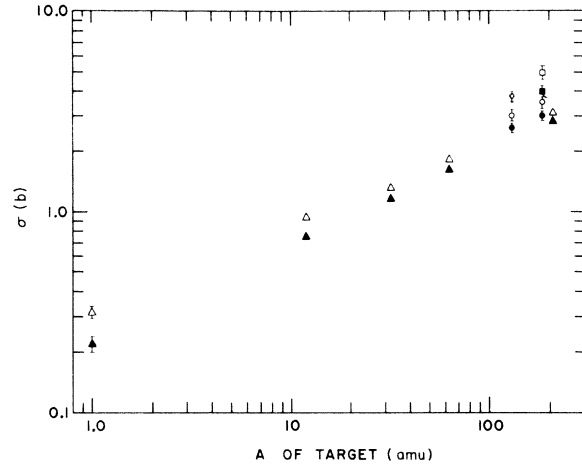


FIG. 6. Total fragmentation cross section σ as a function of mass number of the target nucleus, for incident ^{12}C nuclei (closed symbols) and ^{16}O nuclei (open symbols). Results from this experiment: \bullet and \circ . Results from Ref. 11: \blacktriangle and \triangle . Results from Ref. 12: \blacksquare and \square . Results from Ref. 13: \diamond .

rections arises from two sources:

(a) Uncertainties of typically $\pm 7\%$ in the ratio of the partial ($\Delta Z = 1$) cross section to the total cross section. However, the magnitude of the correction is at most 10% (for the 4.5-FWHM window in the tungsten modules), in which case a $\pm 7\%$ error in the ratio is reduced to a $\pm 0.7\%$ error in the corrected value.

(b) Inaccuracies in the energy-loss distributions for $\Delta Z = 1$ interactions. These distributions were obtained by scaling the observed noninteracting particle distributions by the appropriate Z^2 ratios. The error introduced here is difficult to evaluate. A reasonable estimate may be $\pm 10\%$, in which case its contribution to the error in the value being corrected is $\pm 1\%$.

IV. RESULTS

The cross section σ and interaction mean free path λ for each projectile-target combination are

TABLE III. Dependence of the overlap parameter b on the nucleon radius parameter r_0 as calculated from the cross sections measured in this experiment.

r_0 (10^{-13} cm)	$^{12}\text{C}-\text{CsI}$	$^{12}\text{C}-\text{W}$	$^{16}\text{O}-\text{CsI}$	$^{16}\text{O}-\text{W}$
1.0	-1.77 ± 0.20	-1.81 ± 0.19	-2.23 ± 0.32	-2.33 ± 0.46
1.1	-0.95 ± 0.18	-0.92 ± 0.22	-1.34 ± 0.29	-1.38 ± 0.42
1.2	-0.25 ± 0.17	-0.18 ± 0.16	-0.60 ± 0.26	-0.58 ± 0.38
1.3	0.33 ± 0.16	0.45 ± 0.15	0.03 ± 0.25	0.10 ± 0.35
1.4	0.83 ± 0.15	0.99 ± 0.14	0.57 ± 0.23	0.68 ± 0.33
1.5	1.27 ± 0.13	1.45 ± 0.13	1.04 ± 0.21	1.18 ± 0.31

TABLE IV. Values of the nucleon radius parameter r_0 which are consistent with the overlap parameter $b = 0$ as calculated from the cross sections measured in this experiment.

	$^{12}\text{C}-\text{CsI}$	$^{12}\text{C}-\text{W}$	$^{16}\text{O}-\text{CsI}$	$^{16}\text{O}-\text{W}$
r_0 (10^{-13} cm)	1.24 ± 0.03	1.23 ± 0.03	1.29 ± 0.05	1.28 ± 0.06

presented in Table I. The error quoted for each value includes errors associated with the corrections discussed in the preceding section and the error obtained in the maximum-likelihood calculation. Since the individual errors were added in quadrature, the total error is determined almost entirely by the error obtained in the maximum-likelihood calculation.

The data have been analyzed using window widths of 2.5, 3.5, and 4.5 times FWHM of the noninteracting particle distribution for each module. The cross section σ is given as a function of window width for each projectile-target combination in Table II, both with and without corrections for interactions simulated by pulse height fluctuations as discussed in the preceding section. As expected, the uncorrected cross sections are higher for the narrower windows because of the greater probability for pulse height fluctuations out of the windows. The cross sections obtained after applying corrections are essentially independent of window width for tungsten, but show a small divergence or spread in values for CsI. This variation is probably due to inexact noninteracting particle distributions used in the corrections. The values for σ and λ quoted in Table I for each projectile-target combination are the mean values of the results obtained for each of the three window widths, with corrections applied for interactions simulated by fluctuations in energy losses in the individual modules.

Total fragmentation cross sections ($\Delta Z \geq 1$) for incident ^{12}C and ^{16}O nuclei, obtained in this and other experiments, have been plotted in Fig. 6 as a function of atomic mass number of the target nucleus. The data of Lindstrom *et al.*¹¹ can be fitted with two straight lines on the log-log plot, *i.e.*, σ is given by a power law of the form $\sigma = aA^b$, with $a = 0.24$ and $b = 0.46$ for an incident ^{12}C , and $a = 0.31$ and $b = 0.43$ for an incident ^{16}O .

Our values at $A = 184$ (tungsten) lie somewhat above these straight lines, but are lower than the values obtained by Balasubrahmanyam *et al.*¹² and by Verma and Herzo.¹³

The total interaction cross sections measured in this experiment can be used to calculate the overlap parameter b in the expression proposed by Bradt and Peters¹⁴

$$\sigma_{pt} = \pi r_0^2 (A_p^{1/3} + A_t^{1/3} - b)^2,$$

where A_p and A_t are, respectively, the atomic mass numbers of the projectile nucleus and the target nucleus. The parameter r_0 characterizes the geometrical radius of a nucleus with atomic mass number A according to the relationship $R_{\text{geom}} = r_0 A^{1/3}$. Various values for r_0 have been quoted. Generally, r_0 is taken to be in the range $(1.15-1.45) \times 10^{-13}$ cm. Clearly, the value obtained for b will depend on the value chosen for r_0 . In Table III we show the dependence of b on values of r_0 in the range $(1.0-1.5) \times 10^{-13}$ cm, using the cross sections quoted in Table I. The value of r_0 consistent with $b = 0$, for each projectile-target combination, is given in Table IV.

V. CONCLUSIONS

The analysis described in this paper has been based on a one-module criterion for determining the location of an interaction. The results are independent of the windows used, provided corrections are made for interactions simulated by energy loss fluctuations in the individual modules and for $\Delta Z = 1$ interactions missed because of the use of wide windows. The cross sections obtained are in general agreement with the values obtained in other experiments for various target nuclei. For our cross sections and $r_0 = 1.25 \times 10^{-13}$ cm, calculated values for the overlap parameter b are consistent with zero for each projectile-target combination.

*Research supported by NASA Contracts Nos. NAS5-11426, NAS5-11425, NAS8-27408, NAS9-10986, NAS9-11884, NASA Grant No. NGR 19-001-012, by the U.S. National Science Foundation, and by German Science Ministry Grant No. WRK-244.

†Present address: Service de Physique Nucléaire,

University Libre de Bruxelles, Bruxelles 5, Belgium.

‡Present address: Physics Department, Texas A&M University, College Station, Texas 77840.

§Also Institute of Atmospheric Physics, University of Arizona.

¶M. M. Shapiro and R. Silberberg, *Annu. Rev. Nucl.*

- Sci. 20, 323 (1970).
- ²F. Yiou, *Ann. Phys. (Paris)* 3, 169 (1968).
- ³J. A. Simpson, in *Twelfth International Conference on Cosmic Rays, Hobart, 1971, Invited and Rapporteur Papers*, edited by A. G. Fenton and K. B. Fenton (Univ. of Tasmania Press, Hobart, Tasmania, 1971), p. 324.
- ⁴W. R. Webber, J. A. Lezniak, J. C. Kish, and S. V. Damle, *Nat. Phys. Sci. (Lond.)* 241, 96 (1973).
- ⁵J. F. Ormes and V. K. Balasubrahmanyam, *Nat. Phys. Sci. (Lond.)* 241, 95 (1973).
- ⁶L. H. Smith, A. Buffington, G. F. Smoot, L. W. Alvarez, and M. A. Wahlig, *Astrophys. J.* 180, 987 (1973).
- ⁷E. Juliusson, P. Meyer, and D. Müller, *Phys. Rev. Lett.* 29, 445 (1972).
- ⁸W. A. Fowler, J. L. Greenstein, and F. Hoyle, *Geophys. J. R. Astron. Soc.* 6, 148 (1962).
- ⁹W. V. Jones, K. Pinkau, U. Pollvogt, W. K. H. Schmidt, and R. W. Huggett, *Nuovo Cimento* A8, 575 (1972).
- ¹⁰H. Crannell, C. J. Crannell, H. Whiteside, J. F. Ormes, and M. J. Ryan, *Phys. Rev. D* 7, 730 (1973).
- ¹¹P. J. Lindstrom, D. E. Greiner, and H. H. Heckman, *Bull. Am. Phys. Soc.* 17, 488 (1972).
- ¹²V. K. Balasubrahmanyam, C. J. Crannell, F. A. Hagen, J. F. Ormes, and M. J. Ryan, in *Twelfth International Conference on Cosmic Rays, Hobart, 1971, Conference Papers*, edited by A. G. Fenton and K. B. Fenton (Univ. of Tasmania Press, Hobart, Tasmania, 1971), Vol. 3, p. 1207.
- ¹³S. D. Verma and D. Herzo, in *Thirteenth International Conference on Cosmic Rays, Denver, 1973, Conference Papers* (Colorado Associated Univ. Press, Boulder, 1973), Vol. 4, p. 2883.
- ¹⁴H. L. Bradt and B. Peters, *Phys. Rev.* 77, 54 (1950).